Surface properties of amorphous nanoporous GeS_2

G. Ori[1,2], M. Celino[3], C. Massobrio[4], and B. Coasne[1,2,5]

[1]Institut Charles Gerhardt, CNRS-UMR 5253, University of Montpellier II, ENSCM, Montpellier, France
[2]MSE2, CNRS-MIT UMI 3466, Cambridge, MA, USA, guidoori@mit.edu
[3]Dipt. Technologie Fisiche e Nuovi Materiali, ENEA, Roma, Italy, massimo.celino@enea.it
[4]IPCMS, CNRS-UMR 23, Strasbourg Cedex 2, France, carlo.massobrio@ipcms.unistra.fr
[5]Dept. of Civil Environmental Engineering, Massachusetts Institute of Technology, MA, USA, coasne@mit.edu

ABSTRACT

In this work molecular simulations are used to probe the gas adsorption properties of amorphous chalcogenide nanopores. A realistic atom-scale model, derived by first-principles calculations, of glassy chalcogenide surface is considered for the present study. Nitrogen adsorption and condensation at 77 K in pores of different widths are simulated for characterization purposes. The adsorption of carbon dioxide, methane, hydrogen, and their mixtures is investigated at 298 K. Analysis of the adsorption data shows nice agreement with the prediction of obtained using the Ideal Adsorbed Solution Theory. A detailed comparison with experimental literature data is also proposed and discussed. We also address the effect of the surface chemistry on the gas adsorption by studying both bare and hydrogenated chalcogenide surfaces. We show here that porous glassy chalcogenide exhibits highly selective gas adsorption properties and can strongly discriminate among gases on the basis of their interaction with the chalcogenide surface.

Keywords: glasses, porous chalcogenide, molecular simulation, gas separation, CO_2 capture

1 INTRODUCTION

Gas separation and purification have the potential to play a relevant role in creating large-scale changes to the mix of energy sources currently used by our global society (i.e., hydrogen purification).[1] The challenge of developing effective separation and purification technologies that have much smaller energy footprints is greater for carbon dioxide (CO_2) than for other gases.

Porous materials, such as gels, thanks to their properties based on high surface area and adsorption capacities are relevant to efficient gas separations and therefore critical to energy utilization and emerging clean energy technology.[2] Porous materials, typically made of metal oxides, carbon, or metal-organic frameworks (MOF), have recently been expanded to include the emerging new chalcogenide materials called chalcogels.[3], [4] Chalcogels feature random amorphous networks similar to those of amorphous silica. Because of the soft nature of chalcogen elements (S, Se, and Te), the polarizability of the internal surface of chalcogels is much higher than those of metal oxides and porous carbons and therefore provides an entirely new medium through which to study separation of gases. Molecular simulations have proven to be an efficient technique to investigate the physics of gas adsorption on solid surfaces. In particular, Grand Canonical Monte Carlo simulations (GCMC) have proven to be a suitable technique to achieve an atom-scale understanding of the physical phenomena involved during adsorption of various gas on porous silica and carbon, in nice agreement with both experiment and theory.[5]

The present work aims at looking at the gas adsorption properties of a porous material made of glassy GeS_2 (g-GeS_2, g standing hereafter for glass). GCMC simulations are employed to investigate the adsorption of nitrogen (N_2), for characterization purposes, carbon dioxide (CO_2), hydrogen (H_2), methane (CH_4) and their mixture in g-GeS_2 pores. Here we used a realistic model g-GeS_2 surface recently developed by means of first-principles calculations from a bulk model.[6], [7] We also investigate the effect of surface chemistry by considering both bare and hydrogenated g-GeS_2 surfaces. The study of a hydrogenated chalcogenide, as film or porous material, is relevant to its final application.[8]

2 METHOD AND COMPUTATIONAL DETAILS

Two models of porous chalcogenide have been used in this work: a bare and a hydrogenated chalcogenide. The model of bare g-GeS_2 was obtained by means of first-principles molecular dynamics. Details of the procedure used can be found in Ref. 6 and 7. This realistic model of GeS_2 surface contains 480 atoms and has a size of $2.358 \times 2.358 \times 2.358$ nm^3 with 1.2 nm along the z direction of free volume on the top and the bottom. The bare chalcogenide pore was obtained as follows: by applying periodic boundary conditions along the three directions (x, y, z) the model is characterized by two (different) opposite surfaces replicated infinitely along the x and y axes. This system was replicated 2×2 times along the xy plane. Note that the width of our pores (H) is defined as the distance between the mean positions of the S and Ge of each facing (along the z axes) surface. A nanopore with width $H = 3.6$ nm was obtained by inserting $4.716 \times 4.716 \times 1.20$ nm^3 vac-

CTSI-Cleantech 2014, www.ct-si.org, ISBN 978-1-4822-5819-6

uum slab in between the facing chalcogenide surfaces. To build a hydrogenated g-GeS_2 surface, the undercoordinated (with less than two neighbors) S atoms located at a distance < 0.5 nm from the surface were saturated by hydrogen atoms. In so doing, the final thiol surface density is $\sim$2.3 SH/nm^2. The Ge-S-H and S-S-H angles were obtained by DFT calculations performed for several sub-units (Ge_xS_y clusters of < 20 atoms) taken from the original g-GeS_2 surface model. The electronic structure was described using the DFT theory with the BLYP functional in the frame of generalized gradient approximation for the exchange and correlation parts of the total energy.[9], [10] The DFT calculations were performed with the CPMD code.[11] Computational details can be found in Ref. 6. Nitrogen was described using the model of Potoff and Siepmann (TraPPE forcefield).[12] The rigid model by Harris and Yung,[13] which has been fitted to reproduce the experimental vapor-liquid equilibrium and dynamical properties of bulk CO_2, was used in this work to describe the carbon dioxide molecule. Molecular H_2 and CH_4 are treated as single spherical particles. In our simulations, the methane and hydrogen molecules are simply described as a single Lennard-Jones sphere. All the interactions between the atoms of the adsorbate molecules (N_2, CO_2, CH_4, and H_2) and the Ge, S, H atoms were calculated by considering the intermolecular energy as the sum of the Coulombic and dispersion interactions with a repulsive short-range contribution. The Ge, S and H atoms of the chalcogenide models are described as Lennard-Jones spheres with parameters (ϵ and σ) from Ref. 14 and 15 for Ge and S plus a set of electrostatic charges. Following our previous work, the atomic partial charges on the Ge and S atoms of g-GeS_2 were derived using the Qeq method.[16] In this method, the atomic Ge and S partial charges are derived as a function of their local coordination (for details see Ref. 7). For the hydrogenated surface, the potential parameters and partial charge for the H atoms were taken from Ref. 15. The intermolecular interaction energy between various sites in adsorbates and chalcogenide atoms are calculated through a Coulombic electrostatic contribution and a pairwise-additive Lennard Jones (LJ) 12-6 potential. In our simulations, the LJ cross interaction parameters (σ_{ij}, ϵ_{ij}) between unlike sites are calculated using the Lorentz-Berthelot mixing rules. Periodic boundary conditions were used in the simulations. The dispersive interactions were neglected past a cutoff of 15 Å. The electrostatic interactions were computed using the Ewald summation technique to correct for the finite size of the simulation box (the parameters were chosen so that the accuracy is 10^{-5}). The potential form used in this work reproduces a surface charge distribution dependent on the local environment for Ge and S atoms. This charge assignment is particularly suitable for the present study because it describes

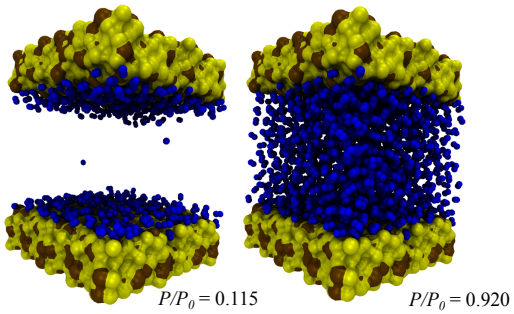

Figure 1: (Color online) Typical molecular configurations for nitrogen in the bare chalcogenide pore with H = 3.6 nm: 0.115 P/P_0 (left) and 0.920 P/P_0(right). The ochre and yellow spheres are the Ge and S atoms of the chalcogenide surfaces, respectively. Th blue spheres are the nitrogen molecules.

the charge distribution as a function of the chemical order, which for the case of glassy chalcogenides can differ discretely from the perfect chemical order.[7] We performed GCMC simulations of nitrogen adsorption at 77 K (for characterization purposes) as well as carbon dioxide, methane, and hydrogen at 298 K in bare and hydrogenated chalcogenides. We also considered the coadsorption of carbon dioxide-methane and carbon dioxide-hydrogen mixtures with bulk compositions of 50-50%. The GCMC technique is a stochastic method that simulates a system having a constant volume V (the pore with the adsorbed phase) in equilibrium with an infinite reservoir of molecules imposing its chemical potential μ_S on each species (S = N_2, CO_2, CH_4, and H_2) at temperature T.

3 RESULTS AND DISCUSSION

The structural and electronic properties of the bare g-GeS_2 surface are reported in our previous study.[7] The g-GeS_2 surface shows a slightly lower chemical order with respect to bulk g-GeS_2,[6] although it shows a similar main tetrahedral structural motif. To characterize the sample further, here, N_2 adsorption at 77 K is performed by means of GCMC simulations. N_2 adsorption is a widely used technique to characterize the surface area and porosity of materials. We studied the adsorption isotherms for bare and hydrogenated g-GeS_2 nanopores with several widths. Here we discuss the results obtained for nanopores with H = 3.6 nm.

The data obtained conform to the typical behavior observed in the experiments of adsorption/condensation in solid nanopores; the adsorbed content increases continuously in the multilayer adsorption regime until a jump occurs because of capillary condensation of the N_2 within the pore. The condensation pressures is $\sim$0.67 P/P_0. The data obtained conform to the experimen-

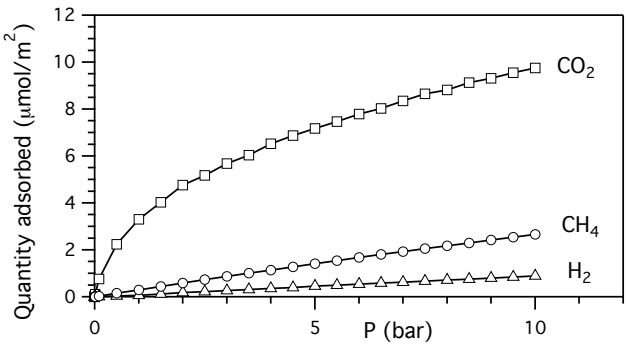

Figure 2: CO_2 (cubes), CH_4 (circles), and H_2 (triangles) adsorption isotherms for bare g-GeS_2 at 298 K. The data are shown for the pore with $H = 3.6$.

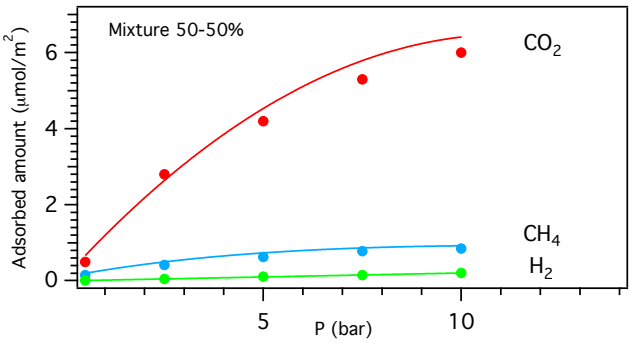

Figure 3: (Color online) Simulated coadsorption of CO_2/CH_4 and CO_2/H_2 at 298 K. The bulk composition of the CO_2-$CH_4(H_2)$ mixture are 50-50%. The solid lines are predictions obtained from the simulated adsorption isothems obtained by the IAST theory (see text).

tal behavior for adsorption/condensation obtained by Kanatzidis et al.[4] Independently of the pore width the surface of g-GeS_2 nanopores is covered with a homogeneous film at the onset of capillary condensation. A discontinuous transition between the partially filled and completely filled configurations occurs when the adsorbed film becomes unstable, in line with the experimental data. Figure 1 shows typical molecular configurations of nitrogen adsorbed at different pressures upon adsorption in the nanopore with $H = 3.6$ nm. At low pressure ($\sim$0.115 P/P_0) the chacogenide surface is covered with a homogeneous film of N_2. At $\sim$0.920 P/P_0 the g-GeS_2 nanopore is completely filled. The hydrogenated g-GeS_2 nanopores show similar trend for all the pore widths (data not shown). The only appreciable difference is a lower adsorption ($\sim$ -5%) of N_2 at the low pressure (< 0.02 P/P_0). This result can be attributed to a weaker interaction between N_2 molecules and the hydrogen atoms of the surface with respect the sulfur atoms. This result shows that a small variation (intended as contamination or functionalization) of the surface chemistry of g-GeS_2 causes an effect on the adsorption properties.

All the CO_2, CH_4 and H_2 adsorption isotherms in this work were simulated at 298 K in order to investigate gas adsorption at a temperature of practical interest. Figure 2 shows the adsorption isotherm for CO_2, CH_4, and H_2 in the bare g-GeS_2 nanopores with $H = 3.6$ nm. For CO_2 the adsorption amount increases rapidly with increasing the pressure and then the slope decreases as the pores get filled. For CH_4 and H_2, the adsorption amount increases almost linearly with the pressure. The adsorption isotherms for CO_2, CH_4 and H_2 of g-GeS_2 indicate a significantly higher affinity for CO_2 compared with CH_4 and H_2. The stronger affinity CO_2 for the g-GeS_2 surface can be ascribed to the favorable interactions between quadrupole of CO_2 (here represented by the partial charges attributed to the oxygen and carbon atoms) and the g-GeS_2 surface atoms. For CO_2, the adsorbed amount does not differ significantly with increasing the the pore width. In contrast, a small increase with increasing the pore width can be noted for CH_4. For H_2, this effect is significant. This result can be ascribed to the stronger affinity of CO_2 for the g-GeS_2 surface in comparison to CH_4 and H_2. The almost perfect linearity of the adsorbed content with increasing the pressure for H_2 suggests a very weak interaction with the g-GeS_2 surface. This observation is in accordance with the fact that H_2 content increases almost linearly with increasing the pore volume; the H_2 adsorbed content in g-GeS_2 nanopores corresponds to the content in equilibrium with the gas phase at a given pressure and temperature. For CH_4 an intermediate behavior can be noted; only a small effect of the pore width on the CH_4 adsorbed content can be noted with increasing the pressure. Overall, the simulated data conform qualitatively to the experimental isotherms obtained by Kanatzidis et al.[4] for a chalcogel with S:Ge_9 $\sim$1.9. The differences between our simulated results and the experimental data can be ascribed to the different S:Ge ratio, where the higher S content of our model could explain the higher adsorption of CO_2 due to the polarizable nature of S. As for the case of N_2 adsorption, CO_2, CH_4, and H_2 adsorption isotherms for the hydrogenated nanopores indicate an overall decrease on gas adsorption with respect to the bare g-GeS_2 nanopores. In particular, the decreases in gas adsorption are $\sim$-12%, $\sim$-11%, and $\sim$-7% for CO_2, CH_4, and H_2, respectively. These values indicate that the interaction between the adsorbates and the surface hydrogen atoms is weaker than with the sulfur atom of g-GeS_2. This effect is more pronounced for the gas adsorption of CO_2 and CH_4 than of H_2. This result is consistent with the fact that the

interaction of CO_2 with the g-GeS_2 surface is stronger than those of CH_4 and H_2, thus is more affected by the presence of hydrogen atoms on the g-GeS_2 surface. We also performed GCMC simulations of the coadsorption of CO_2/CH_4 and CO_2/H_2 mixtures in the bare g-GeS_2 nanopore with width $H = 3.6$ nm. Figure 3 shows the simulated coadsorption isotherms. The bulk molar composition of CO_2/CH_4 and CO_2/H_2 mixtures studied in this work is 50-50%. The maximum adsorbed contents of CO_2 at $P = 10$ bar and $T = 298$ K is 5.9 μmol/m^2 for CO_2. For CO_2/H_2 mixtures the maximum adsorbed amounts of CO_2 at the same P and T is 6.0 μmol/m^2 for the same bulk composition. We show also in Figure 2 the predictions obtained using the ideal adsorbed solution theory (IAST)[17], which is widely used to predict the adsorption of mixtures from the data of the pure components. IAST assumes that the adsorbed mixture is an ideal solution. The GCMC simulations and the predicted theoretical values are in good agreement. The discrepancy between the simulated and predicted data can be ascribed to the fact that the IAST does not take into account adsorbate-adsorbate interaction in the adsorbed phase.

4 Conclusions

GCMC simulations of gas (N_2, CO_2, CH_4, and H_2) adsorption in g-GeS_2 nanopores are reported and discussed. Thanks to the realistic quality of the g-GeS_2 model used in this work, we are able to compare the adsorption properties simulated in this work with experimental data from literature. The characterization of the adsorption properties of g-GeS_2 by means of N_2 adsorption at 77 K shows the typical behavior observed in the experiments of adsorption/condensation in solid nanopores. We found a N_2 condensation pressure in nice agreement with the GeS-based chalcogel synthesized the group of Kanatzidis for a similar pore size. This result further proves the realistic quality (in terms of surface structure and charge distribution) of the g-GeS_2 nanopore models investigated in this work. By investigating the adsorption isotherms of g-GeS_2 nanopores for CO_2, CH_4, and H_2, a stronger interaction for CO_2 with the g-GeS_2 surface is highlighted with respect to CH_4 and H_2. H_2 shows a very weak affinity with the g-GeS_2 surface, thanks to which the H_2 adsorption increases linearly as a function of the pore width for higher pressures. The simulations of the adsorption of CO_2/CH_4 and CO_2/H_2 mixtures show a relevant selective adsorption of CO_2 over CH_4 and H_2. The results obtained are well described by the ideal adsorption solution theory. We also addressed the study of the effect of the surface chemistry by studying the adsorption in hydrogenated chalcogenide nanopores. The hydrogenation of chalcogenide surfaces causes a small decrease of N_2 adsorption at 77 K at low pressure and a small decrease in the adsorption at 298 K for CO_2 over both CH_4 and H_2.

While further work is needed to clarify the gas adsorption on chalcogenide pores with different shape and surface chemistry, the results above help better understanding the interactions between adsorbates and g-GeS_2 nanopores. The present work shows how glassy porous chalcogenide represent a valuable material for gas separation, especially for the CO_2/H_2 mixture.

REFERENCES

[1] P. Taylor, "Energy Technology Perspectives 2010 - Scenarios and Strategies to 2050", International Energy Agency, Paris, 74, 2010.

[2] P. Nugent, Y. Belmabkhout, S. D. Burd, A. J. Cairns, R. Luebke, K. Forrest, T. Pham, S. Ma, B. Space, L. Wojtas, M. Eddaoudi, and M. Zaworotko, Nature Lett. 495, 80, 2013.

[3] K. K. Kalebaila, D. G. Georgiev, and S. L. Brock, J. Non-Cryst. Solids 352, 232, 2006

[4] G. A. Armatas, and M. G. Kanatzidis, Nature Mater. 8, 271, 2009.

[5] B. Coasne, F. R. Hung, R. J.-M. Pellenq, F. R. Siperstein, and K. E. Gubbins, Langmuir 22, 194, 2006.

[6] M. Celino, S. Le Roux, G. Ori, B. Coasne, A. Bouzid, M. Boero, and C. Massobrio, Phys. Rev. B 88, 174201, 2013.

[7] G. Ori, M. Celino, A. Bouzid, M. Boero, C. Massobrio, and B. Coasne, *submitted*.

[8] A. K. Wesley, A. G. Clare, and W. C. LaCourse, J. Non-Cryst. Solids 181, 231,1995.

[9] A. D. Becke, Phys. Rev. A 38, 3098,1988.

[10] C. Lee, W. Yang, R. G. Parr, Phys. Rev. B 37, 785, 1988.

[11] CPMD, http://www.cpmd.org/, Copyright IBM Corp, 1990-2008, Copyright MPI, Stuttgart 1997-2001.

[12] J. J. Potoff, and J. I. Siepmann, AIChE 47, 1676, 2001.

[13] J. Harris, and K. H. Yung, J. Phys. Chem. 99, 12021, 1995.

[14] S. L. Mayo, B. D. Olafson, and W. A. Goddard, J. Phys. Chem. 94, 8897, 1990.

[15] G. A. Kamiski, R. A. Friesner, J. T.-R., and W. Jorgensen, J. Phys. Chem. B 105, 6474, 2001.

[16] A. K. Rappe, and W. A. Goddard III, J. Phys. Chem. 95, 5, 1991.

[17] A. L. Myers, and J. M. Prausnitz, AIChE 11, 121, 1965.